Soft Matter

PAPER

View Article Online
View Journal | View Issue

Cite this: *Soft Matter*, 2014, **10**, 8023

The evolution of self-assemblies in the mixed system of oleic acid–diethylenetriamine based on the transformation of electrostatic interactions and hydrogen bonds†

Chengcheng Zhou,[b] Xinhao Cheng,[a] Oudi Zhao,[a] Shuai Liu,[a] Chenjiang Liu,[b] Jide Wang[b] and Jianbin Huang*[ab]

Received 4th June 2014
Accepted 28th July 2014

DOI: 10.1039/c4sm01204f

www.rsc.org/softmatter

With the aid of pH variation, the fine control of the electrostatic interaction and hydrogen bond was realised in the mixed system of oleic acid and diethylenetriamine. Owing to the transformation of the intermolecular interactions, the corresponding building blocks changed from $DETA^{2+}@2OA^{-}$ *via* the coexistence of $DETA@2OA^{-}$ and $DETA^{+}@OA^{-}$ to $DETA@2OA^{-}$. Therefore, diverse microstructures and phase behaviors in this mixed surfactant system were obtained at the different pH values. It is found that the fine control of the electrostatic interaction and hydrogen bond is efficient for tailoring the self-assembled structures in this cationic–anionic surfactant system, including vesicles, bilayers, networks formed by aggregated vesicles and fibers.

Introduction

Molecular self-assembly driven by the noncovalent interactions, a ubiquitous process in chemistry, biology and materials science, provides the foundation for building well-defined structures in the nanometer or micrometer length scale.[1,2] Based on the rational control of the noncovalent interactions,[3] such as hydrogen bonds,[4,5] electrostatic forces, van der Waals forces, hydrophobic interactions, dipole–dipole interactions and π–π stacking,[6] a variety of self-assembled structures such as tubules, fibers, micelles, vesicles and lamellae have been fabricated.[7–11] In contrast to the single system, the mixture of anionic and cationic surfactants ("catanionic" mixed surfactant system) is more favorable in constructing complex self-assembled structures and in practical applications.[12,13] Therefore, the "catanionic" surfactant systems have been drawing increasing attraction. However, finely controlling the construction of the self-assemblies and understanding the relationship between the organized assemblies and the noncovalent interactions in the "catanionic" surfactant systems is still one of the most important challenges facing modern chemistry.[14,15]

For the catanionic surfactant systems, the molecular self-assemblies are mainly attributed to the strong electrostatic attraction between the oppositely charged headgroups.[16,17] The construction and evolution of the self-assemblies in the catanionic surfactant system generally depends on control of the electrostatic interaction by varying the surfactant ratio,[18,19] modifying solvent properties[20–22] or adding an inorganic salt.[23] In contrast, the effects of the other noncovalent interactions on the transformation of the self-assemblies in this kind of mixed system are studied rarely, based on the viewpoint that the variation of the other noncovalent interactions may be not strong enough to induce the transformation of the self-assemblies in the presence of the electrostatic interaction. Recently, the studies by our group demonstrated that the aggregate transition can be tuned by external factors such as temperature, light and pH in the catanionic surfactant systems which were mainly governed by electrostatic interactions.[11,24–28] This gave us a hint that the other weak interactions besides the electrostatic interaction can also play an important role in catanionic surfactant systems, which may generate a new approach to advance the research in this field.

Herein, we studied the evolution of self-assemblies based on the transformation of the electrostatic interaction and hydrogen bond in the mixed systems of oleic acid–diethylenetriamine. Two pH-responsive molecules, oleic acid (OA) and diethylenetriamine (DETA), were selected to fabricate self-assembled constructions in this "catanionic" surfactant system. With the increase of pH, the molecular interactions transformed sequentially from the strong electrostatic attraction, through the coexistence of weak electrostatic attraction and hydrogen

[a]*Beijing National Laboratory for Molecular Sciences (BNLMS), State Key Laboratory for Structural Chemistry of Unstable and Stable Species, College of Chemistry and Molecular Engineering, Peking University, Beijing 100871, China. E-mail: jbhuang@pku.edu.cn*

[b]*College of Chemistry and Chemical Engineering, Xinjiang University, Urumqi 830046, China*

† Electronic supplementary information (ESI) available. See DOI: 10.1039/c4sm01204f

bonds to the coexistence of electrostatic repulsion and hydrogen bonds. Simultaneously, the corresponding building blocks are controlled from $DETA^{2+}@2OA^{-}$ *via* coexistence of $DETA@2OA^{-}$ and $DETA^{+}@OA^{-}$ to $DETA@2OA^{-}$ at different pH values. As a result, the aggregate morphologies transform from the micron-sized giant vesicles *via* the coexistence of small vesicles and bilayers to a network formed by the aggregated vesicles. In addition, when the electrostatic repulsion is screened and the hydrogen bond becomes the dominant intermolecular interaction by the addition of an inorganic salt, the network structures transform into fibers, accompanied by gel formation.

Experimental section

Materials

Oleic acid (OA, 99.5%) was purchased from Xilong Chemical Co. (Shantou city, Guangdong, China) and used as received. Diethylenetriamine (DETA, 99%) was purchased from Beijing Yili Fine Chemicals Co. (Beijing, China). Ultrapure water was used throughout the work.

Sample preparation

Desired amounts of oleic acid, diethylenetriamine and water were weighed into an Erlenmeyer flask to give the OA–DETA molar ratio of 1 : 1 and the total molar concentration of 30 mM. The samples were vortex mixed sufficiently and aged for at least 24 h to complete the acid–alkali neutralizing reaction. The concentrated sodium hydroxide solution was added to adjust the pH value of the samples. Finally the resultant mixtures were thermostatically incubated at 25 °C (for at least 24 h) before measurements.

TEM observation

The morphology of the self-assemblies was observed using a JEM-100 CX II transmission electron microscope (JEOL, Japan). A drop of sample was placed on 230 mesh copper grids coated with a Formvar film. Excess water was removed with filter paper followed by staining negatively the film with uranyl acetate. After removal of the excess staining liquid by filter paper, the samples were placed at room temperature to dry for TEM observation.

Atomic force microscopy (AFM)

AFM measurements in tapping mode under ambient conditions were conducted on a D3100 AFM (VEECO, USA). One drop of the mixed solution was spin-coated on a mica surface, and then placed at room temperature to dry before AFM observation.

SEM observation

The gel sample was mounted onto a silicon wafer and air-dried before SEM observation (Hitachi S4800, Japan).

Dynamic light scattering (DLS) measurements

DLS measurements were conducted on an ALV/DLS/SLS5022F light scattering-apparatus (ALV/Laser Vertriebsgesellschaft m. b. H Co., Germany) equipped with a 22 mW He–Ne laser (632.8 nm wavelength) with a refractive index matching bath of filtered toluene surrounding the cylindrical scattering cell. The samples were filtered by 450 nm filters. The scattering angle was 90°.

Fourier transform infrared (FT-IR)

FT-IR measurements were performed on a Nicolet iN10 MX equipped with an infrared microspectrometer (Thermo Scientific Co., USA). The samples were dropped on a slide and then allowed to dry at room temperature before FT-IR measurements.

Fourier transform ion cyclotron resonance mass spectrometer (FT-MS)

ESI-MS measurements were carried out on an APEX IV FT-MS (Bruker, USA). The operating conditions of the ESI source: positive ion mode; spray voltage −3300 V; capillary voltage −3800 V, capillary temperature 200 °C; skimmer1 33.0 V, skimmer2 28.0 V; sheath gas nitrogen pressure 0.3 bar. The initial OA–DETA samples for MS measurements: concentration 30 mM; OA–DETA molar ratio 1 : 1; pH 10.5. The pH value of the samples was adjusted to 9.0 and 12.0 by acetic acid and sodium hydroxide solution, respectively. The samples with pH values 9.0, 10.5, 12.0 in water–methanol (10 : 90% v/v) were introduced *via* direct infusion at a flow rate of 3.00 μL min^{-1}.

Rheology measurements

The viscosity of the samples was measured at 25 °C using a Ubbelodhe viscometer.

Results and discussion

Phase behavior of the OA–DETA mixed system with pH variation

Precipitates formed in the OA–DETA mixed systems when pH was below 8.0, therefore, the pH ranging from 8.0 to 12.0 was studied in this work. With the variation of pH, the OA–DETA mixed systems are divided into three regions according to the phase behavior as shown in Fig. 1. In region I (8.0 < pH < 10.0), the mixed systems are of water-like viscosity but high turbidity. With pH ranging from 10.0 to 11.5 (region II), the solutions become transparent and viscoelastic. In region III (pH > 11.5), the mixed systems are still transparent but the viscosity returns to be water-like. In addition, it should also be mentioned that the electrostatic interaction in these mixed systems transformed from strong electrostatic attraction in region I to electrostatic repulsion in region III due to the decreasing ratio of positive and negative charges with pH variation from 8.0 to 12.0 (Table 1). Namely, upon increasing pH, the electrostatic attraction of the mixed systems was gradually weakened and changed into the electrostatic repulsion. On the other hand, the NH vibration of diethylenetriamine moved from 3373 cm^{-1} to 3338 cm^{-1} when pH changed from 9.0 (region I) to 12.0 (region III) as shown in Fig. 2, which demonstrated that the hydrogen bonds were strengthened with the increasing pH in this mixed system.[29,30]

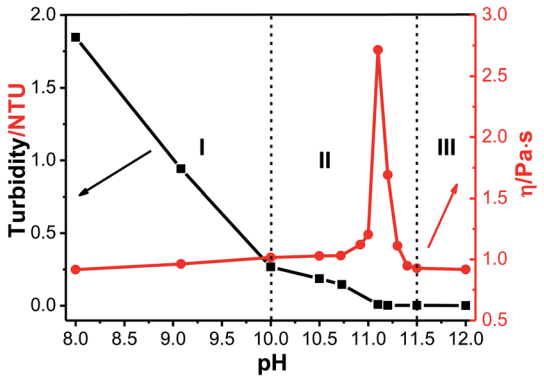

Fig. 1 Variation in turbidity (black line) and viscosity variation (red line) of OA–DETA mixed systems against pH.

Table 1 Species distribution and the ratio of positive and negative charges of the oleic acid–diethylenetriamine mixed system against pH at 25 °C.[31,32] (The species distribution graphs are shown in Fig. S1)

pH	DETA/%	$DETA^{+}$/%	$DETA^{2+}$/%	OA^{-}/%	Charge ratio (+ : −)
8.0	0.06	5.80	88.29	99.87	1.80 : 1
9.0	2.43	32.08	65.49	99.99	1.60 : 1
9.6	23.31	55.92	20.77	100	0.97 : 1
10.0	43.16	48.43	8.42	100	0.65 : 1
10.5	75.98	22.95	1.07	100	0.25 : 1
11.1	88.39	11.39	0.23	100	0.12 : 1
11.3	94.63	5.32	0.05	100	0.06 : 1
11.5	96.23	3.74	0.02	100	0.04 : 1
12.0	98.96	1.04	0.00	100	0.01 : 1

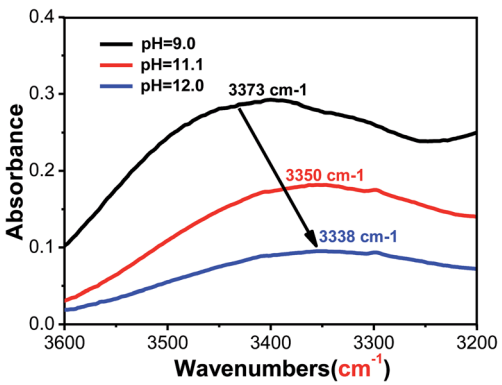

Fig. 2 The IR results of the OA–DETA mixed systems at the different pH values.

According to the above information, the intermolecular interactions of the OA–DETA mixed systems will transform, upon increasing pH, from strong electrostatic attraction (region I) *via* coexistence of weak electrostatic attraction and hydrogen bonds of region II to coexistence of electrostatic repulsion and hydrogen bonds in region III. Then with the different non-covalent interactions, it is clear that the building blocks and the aggregate behaviors of the systems in different regions are remarkably different as will be discussed below.

Formation of giant vesicles in region I (8.0 < pH < 10.0)

In region I (8.0 < pH < 10.0), the OA–DETA mixtures at pH = 9.0 as a typical system were studied. As the pH value of the system reached 9.0, the species $DETA^{2+}$ account for 65.49% of the total diethylenetriamine with oleic acid completely ionized into OA^{-} (Table 1). That is to say that the main species of the mixed systems were $DETA^{2+}$ and OA^{-}. Thus the electrostatic attraction plays the dominant role in this system, which will bring the diverse aggregations. The structure of the self-assemblies in this mixed system was studied by TEM. The TEM image in Fig. 3a presents plenty of micron-sized giant vesicles, which accounts for the high turbidity of this system. There are also some small ones about 50–400 nm according to the DLS results (Fig. S2†). In addition, we can also observe the coexistence of unilamellar and multilamellar vesicles (Fig. 3).

The sample was further studied by AFM in a dehydrate state, as shown in Fig. 4a. AFM images revealed the presence of polydisperse disks with the diameters of 50–400 nm, which is much less than the particle size observed by TEM. This is probably because of the fact that the spin-coated methods resulted in loss of the micron-sized particles. In Fig. 4b and c, we show the sectional height profiles of the collapsed unilamellar and multilamellar vesicles. The height of about 5.1 nm in Fig. 4b was thought to be the thickness of two closely stacked bilayer membranes of the unilamellar vesicle. Considering the symmetric structure of vesicles, this height indicates that the thickness of the unilamellar vesicle shell is about 2.5 nm. Thus the height of 20.1, 10.1 and 15.0 nm can be assigned to the collapsed multilamellar vesicles (Fig. 4b and c). The vesicle shells should correspond to the height of $2n$ building blocks. To determine the main building blocks, MS measurements were carried out for the mixed system.[33–35] The main peaks verified the existence of $DETA^{2+}$@$2OA^{-}$ type building blocks (Table 2). Therefore, in region I, the "pseudo Gemini surfactant" building blocks were fabricated by electrostatic attraction as shown in Scheme 1. The extended length of the building block $DETA^{2+}$@$2OA^{-}$ is about 2.3 nm (Fig. S4a†); twice the building block's size is much larger than the height of bilayer membranes of the unilamellar vesicle. This result strongly suggested that the building blocks $DETA^{2+}$@$2OA^{-}$ form the bilayer structure with strong interdigitation until around the double bond of the oleic acid by hydrophobic interactions (Fig. S4b†).[36,37]

In region I, based on the electrostatic attraction, the "pseudo Gemini surfactant" building blocks were fabricated. Driven by

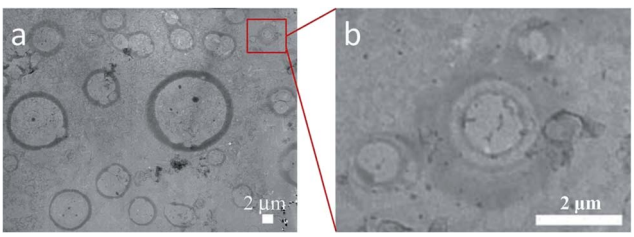

Fig. 3 TEM images of OA–DETA mixed systems at pH = 9.0. (a) The images of the vesicles. (b) Magnification of the multilamellar vesicles.

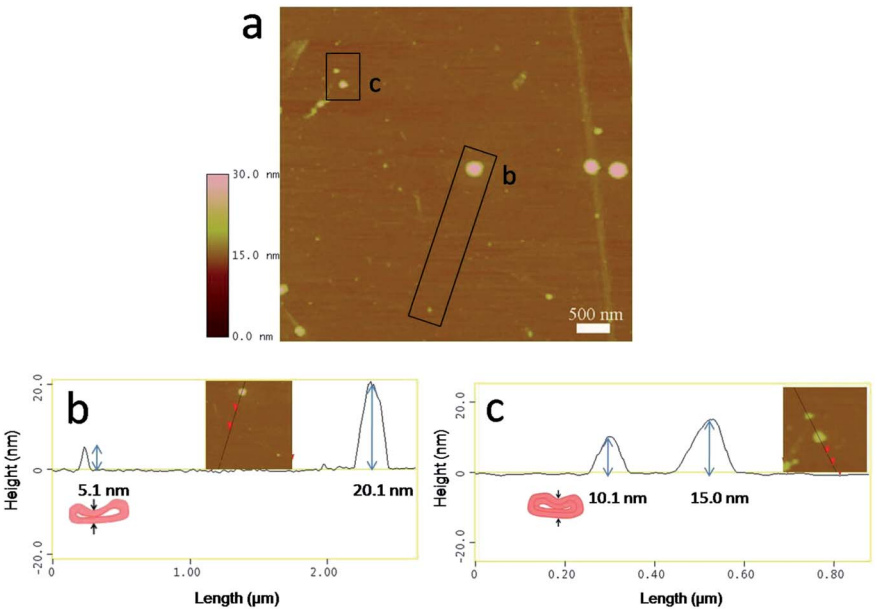

Fig. 4 (a) AFM images of OA–DETA mixed systems at pH = 9.0. (b) and (c) Sectional height profile of the collapsed vesicles chosen in (a).

Table 2 The main MS results at different pH values. (The MS profiles are given in Fig. S3)

pH	Main MS Peak
8.0–10.0 region I	$[(DETA^{2+}@2OA^{-})H\ (DETA^{2+}@CH_3COO^{-})_2(H_2O)_6]^{3+}$ (m/z = 368.36314)
	$[(DETA^{2+}@2OA^{-})_2H\ (DETA^{2+}@CH_3COO^{-})_2(CH_3OH)]^{3+}$ (m/z = 565.51759)
	$[(DETA^{2+}@2OA^{-})H]^{+}$ (m/z = 668.62839)
	$[(DETA^{2+}@2OA^{-})K(CH_3COOH)]^{+}$ (m/z = 766.56147)
	$[(DETA^{2+}@2OA^{-})H(CH_3COOH)_2(H_2O)_2]^{+}$ (m/z = 824.74178)
	$[(DETA^{2+}@2OA^{-})NH_4(DETA^{2+}@2CH_3COO^{-})(H_2O)_3]^{+}$ (m/z = 962.84371)
10.0–11.5 region II	$[(DETA@2OA^{-})Na_4(DETA)(H_2O)_2]^{2+}$ (m/z = 448.28778)
	$[(DETA@2OA^{-})_2Na_4H_2(H_2O)]^{2+}$ (m/z = 721.54196)
	$[(DETA@2OA^{-})_3Na_4H_4(DETA)(CH_3OH)_2]^{2+}$ (m/z = 1129.89012)
	$[(DETA^{+}@OA^{-})K(DETA)]^{+}$ (m/z = 527.43235)
	$[(DETA^{+}@OA^{-})_2K(DETA)(CH_3OH)(H_2O)]^{+}$ (m/z = 962.84889)
	$[(DETA^{+}@OA^{-})_3K(CH_3OH)]^{+}$ (m/z = 1227.09467)
>11.5 region III	$[(DETA@2OA^{-})Na_4(DETA)]^{2+}$ (m/z = 430.33710)
	$[(DETA@2OA^{-})Na_3]^{+}$ (m/z = 734.57273)
	$[(DETA@2OA^{-})Na_3(NaOA)]^{+}$ (m/z = 1038.80695)
	$[(DETA@2OA^{-})Na_3(NaOA)_2]^{+}$ (m/z = 1343.03950)

the electrostatic attraction and the hydrophobic effect, the building blocks self-assemble into unilamellar and multilamellar giant vesicles.

Coexistence of small vesicles and bilayer structures in region II (10.0 < pH < 11.5)

In region II (10 < pH < 11.5), the OA–DETA mixtures at pH = 11.1 as a typical system were studied. From Table 1, the species DETA, $DETA^{+}$ and $DETA^{2+}$ account for 88.39%, 11.39% and 0.23% of the total diethylenetriamine, respectively. Considering the fact that oleic acid is completely ionized into OA^{-} at pH = 11.1, the main species of the mixed systems were DETA, $DETA^{+}$ and OA^{-} in region II. Compared to region I, the electrostatic attraction was weakened and the hydrogen bond was strengthened, which made the phase behaviors and self-assembled structures change. The TEM images in Fig. 5 show the coexistence of vesicles and "lamellae" in this case (please see ESI 5†). The dimensions of the vesicles decreased to 50–400 nm in contrast to the micron-sized giant vesicles of region I. Hence it is reasonable to understand that the turbidity in region II decreases significantly. In addition, we also observed that the adhesion occurred among these small vesicles, which leads to the high viscoelasticity of the mixed systems.

The coexistence of two types of aggregates shows the possibility of the existence of two types of building blocks in region II. Similar to the study in region I, MS measurements were carried out for the mixed system to determine the main building blocks. The main peaks for $[(DETA@2OA^{-})Na_4(DETA)(H_2O)_2]^{2+}$

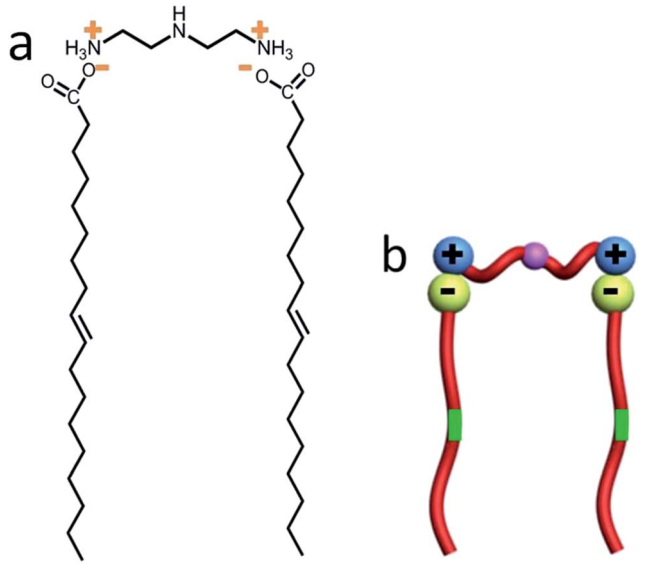

Scheme 1 (a) The building blocks of the OA–DETA mixed systems in region I. (b) The schematic illustration of the building blocks.

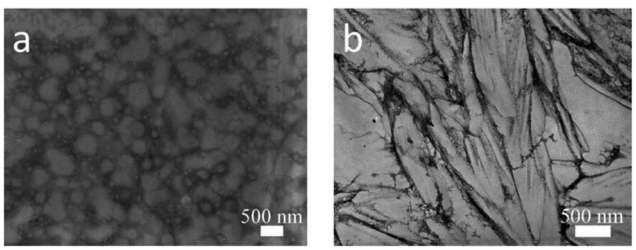

Fig. 5 (a) and (b) TEM images of OA–DETA mixed systems at pH = 11.1 before and after the addition of 5 M urea.

(m/z = 448.28778), $[(DETA@2OA^-)_2Na_4H_2(H_2O)]^{2+}$ (m/z = 721.54196), and $[(DETA@2OA^-)_3Na_4H_4(DETA)(CH_3OH)_2]^{2+}$ (m/z = 1129.89012) in Table 2 confirm the existence of the $DETA@2OA^-$ building blocks. And the peak for $[(DETA^+@OA^-)K(DETA)]^+$ (m/z = 527.43235), $[(DETA^+@OA^-)_2K(DETA)(CH_3OH)(H_2O)]^+$ (m/z = 962.84889), and $[(DETA^+@OA^-)_3K(CH_3OH)]^+$ (m/z = 1227.09467) verified the existence of $DETA^+@OA^-$ building blocks. Therefore, the main building blocks of the OA–DETA mixed system in region II are $DETA@2OA^-$ and $DETA^+@OA^-$ fabricated by the hydrogen bond and the electrostatic attraction, respectively (Scheme 2). Similarly, with the strong interdigitation of the carbon chain until around the double bond of the oleic acid (Fig. S4d and f†), the height of the bilayer membranes formed by building blocks $DETA@2OA^-$ and $DETA^+@OA^-$ is about 2.6 nm and 4.2 nm, respectively. The height of the building blocks should be reflected by the wall thickness of the vesicles and the bilayers of the "lamellae". The AFM images in Fig. 6a further verified the coexistence of vesicles and "lamellae". In Fig. 6c, we show the sectional height profiles of the collapsed vesicle adhesion on the lamellae. The height of the "lamellae" is about 4.2 nm, which are considered as the bilayers from the building blocks $DETA^+@OA^-$. Moreover, the height of the "lamellae" in the whole image is 4.2 nm (Fig. S5†),

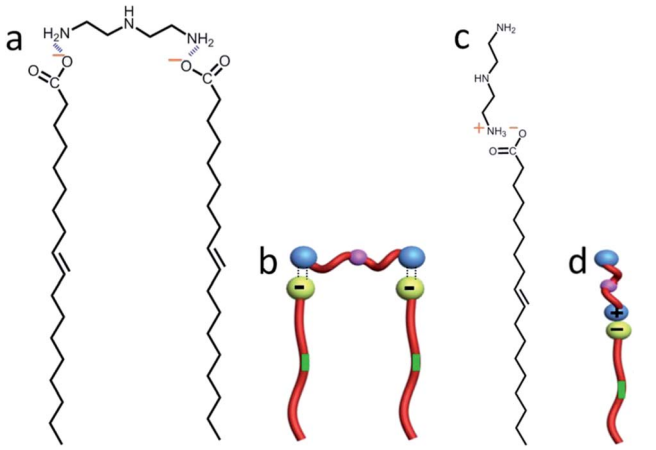

Scheme 2 (a) and (c) The building blocks of the OA–DETA mixed systems in region II. (b) and (d) The schematic illustration of the building blocks.

therefore, the so-called lamellae are actually the bilayers formed by the building blocks $DETA^+@OA^-$. In addition, the height of two disks adhered on the bilayers is about 5.1 nm and 2.5 nm, which is assigned to a collapsed unilamellar vesicle and a broken unilamellar vesicle. This result confirms that the building blocks $DETA@2OA^-$ self-assemble into vesicles.

In short, two types of building blocks $DETA@2OA^-$ and $DETA^+@OA^-$ were fabricated by the hydrogen bond and the electrostatic attraction in the OA–DETA mixed system in region II. The building blocks $DETA@2OA^-$ and $DETA^+@OA^-$ self-assemble into vesicles and bilayers, respectively. The hydrogen bond from the –NH group on the surface of vesicles and the bilayers promoted the adhesion among vesicles and that between vesicles and bilayers, which is responsible for the higher viscoelasticity of region II.

Network formed by the aggregated small vesicle in region III (pH > 11.5)

In region III (pH > 11.5), the OA–DETA mixtures at pH = 12 as a typical system were studied. With the pH value of the system reaching 12, the species DETA take up 98.96% of the total diethylenetriamine with oleic acid completely ionized into OA^- (Table 1). This means that the main species of the mixed systems were DETA and OA^-. In contrast to region II, the hydrogen bond was further strengthened with the weak electrostatic attraction being transformed into the electrostatic repulsion. With the variation of the intermolecular interactions, the phase behaviors and the self-assembled structures changed accordingly. With the aid of TEM and AFM, the structures of the self-assemblies in the OA–DETA mixed systems were observed. The images in Fig. 7a and b show the existence of the network formed by the aggregated vesicles. The dimension of these vesicles is of 100–500 nm, which is similar to that formed in region II.

In Fig. 7c and d, we show that the height difference of the collapsed vesicles is 2.6 and 5.2 nm, which should correspond to the height of $2n$ building blocks. The main peaks of MS

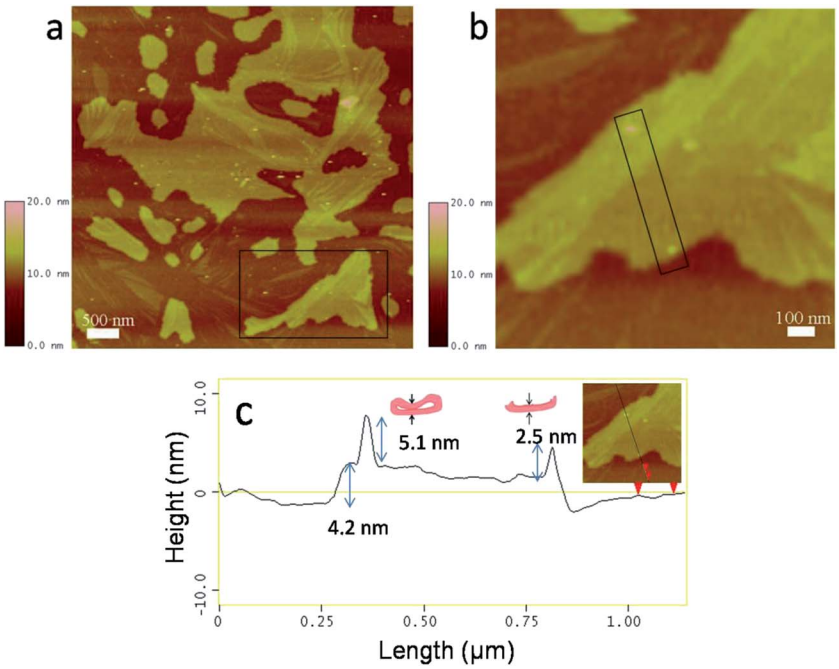

Fig. 6 (a) AFM images of OA–DETA mixed systems at pH = 11.1. (b) The enlarged images of the region chosen in (a). (c) Sectional height profile of the images chosen in (b).

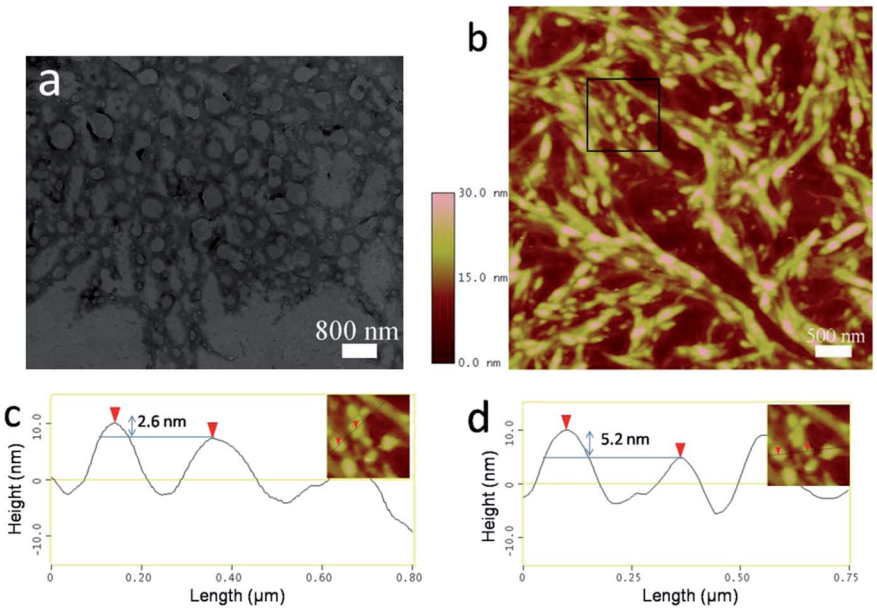

Fig. 7 (a) and (b) TEM and AFM images of OA–DETA mixed systems at pH = 12.0. (c) and (d) Sectional height profile of the images chosen in (b).

measurements confirmed the existence of the DETA@2OA$^-$ building blocks (Table 2). Accordingly, the main building blocks of the OA–DETA mixed system in region III are DETA@2OA$^-$ fabricated by the hydrogen bond (Scheme 3). The height of the bilayer membranes from DETA@2OA$^-$ is about 2.6 nm with strong interdigitation of the carbon chain until around the double bond of the oleic acid (Fig. S4h†), which is consistent with the results of AFM. This further verified that the building blocks DETA@2OA$^-$ fabricated by the hydrogen bond self-assembled into small vesicles. With the bridge effect produced by the NH group on the surface of vesicles and diethylenetriamine molecules in the solution, the vesicles are connected and aggregated into network structures.

In addition, the viscosity of the OA–DETA mixtures decreased from 2.7 to 0.9 Pa s compared with that in region II. This may be attributed to the existence of the electrostatic repulsion in region III. To screen the electrostatic repulsion of the mixed system at pH = 12.0, desired amounts of sodium

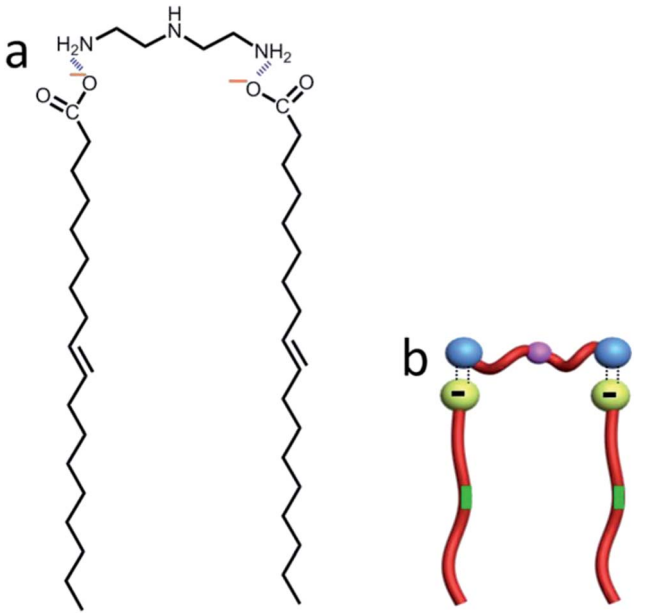

Scheme 3 (a) The building blocks of the OA–DETA mixed systems in region III. (b) The schematic illustration of the building blocks.

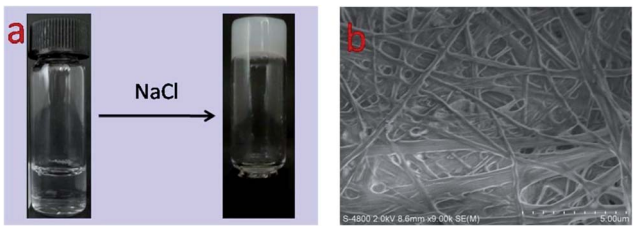

Fig. 8 (a) The macrographs of the OA–DETA mixed system at pH = 12.0 before and after the addition of NaCl. (b) The SEM images of the OA–DETA mixed system at pH = 12.0 after the addition of NaCl.

chloride were added to make the ionic strength be 0.5 mol kg^{-1}. It can be observed that the viscosity increased significantly and the gel was formed after aging for about 10 min (Fig. 8a). The main molecular interactions of the OA–DETA mixed system in region III are electrostatic repulsion and hydrogen bonds. After screening the electrostatic repulsion by the addition of sodium chloride, the hydrogen bond plays the dominant role in this mixed system, which leads to the transformation of self-assembled structures and phase behavior. The SEM images in Fig. 8b show that the gel is composed of fibers, which are mainly driven by the hydrogen bonds.

On the whole, based on the hydrogen bonds, the building blocks DETA@2OA^- were fabricated and assembled into small vesicles due to the hydrogen bonds and electrostatic repulsion in region III. When the hydrogen bond became the dominant intermolecular interaction, the network structures formed by the aggregated small vesicles transformed into fiber structures, accompanied by gel formation.

Conclusion

The fine control of the electrostatic interaction and hydrogen bonds was easily realized in OA–DETA mixtures by pH variation. Based on the transformation of the electrostatic interaction and hydrogen bonds, the corresponding building blocks were fabricated, which account for the evolution of the self-assemblies in this mixed system (Scheme 4). Our studies not only identified the important contribution of hydrogen bonds to the transformation of the self-assemblies in the mixed "cationic–anionic" surfactant systems but also may advance a better understanding of the relationship between the self-assemblies and the weak interactions in this mixed system, which will shed light on the development and application of the self-assembly chemistry.

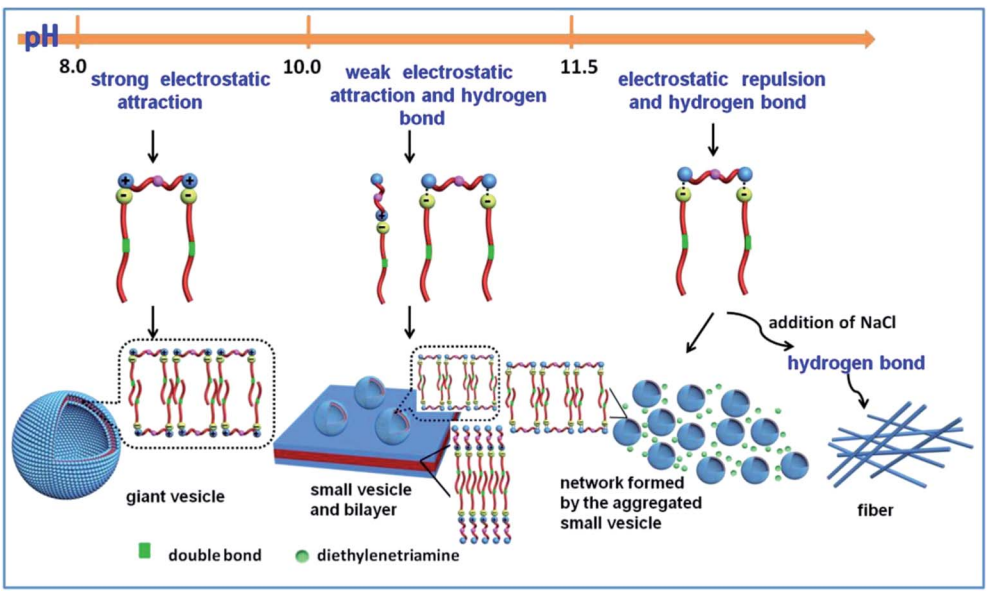

Scheme 4 The schematic aggregate morphology transition of the OA–DETA mixed system with the variation of pH.

Acknowledgements

This work was supported by the Natural Science Foundation of China (21273013), the Foundation for Innovative Research Group of the Natural Science Foundation of China (51121091) and the National Basic Research Program of China (973 Program, 2013CB933800).

Notes and references

1 G. M. Whitesides and B. Grzybowski, *Science*, 2002, **295**, 2418–2421.
2 A. C. Coleman, J. M. Beierle, M. C. Stuart, B. Maciá, G. Caroli, J. T. Mika, D. J. van Dijken, J. Chen, W. R. Browne and B. L. Feringa, *Nat. Nanotechnol.*, 2011, **6**, 547–552.
3 S. Toksoz, H. Acar and M. O. Guler, *Soft Matter*, 2010, **6**, 5839–5849.
4 X. Pei, J. Zhao, Y. Ye, Y. You and X. Wei, *Soft Matter*, 2011, **7**, 2953–2960.
5 R. Iwaura, F. J. M. Hoeben, M. Masuda, A. P. H. J. Schenning, E. W. Meijer and T. Shimizu, *J. Am. Chem. Soc.*, 2006, **128**, 13298–13304.
6 E. Córdova-Mateo, O. Bertran, B. Zhang, D. Vlassopoulos, R. Pasquino, A. D. Schlüter, M. Kröger and C. Alemán, *Soft Matter*, 2014, **10**, 1032–1044.
7 J. Bae, J.-H. Choi, Y.-S. Yoo, N.-K. Oh, B.-S. Kim and M. Lee, *J. Am. Chem. Soc.*, 2005, **127**, 9668–9669.
8 J. H. Fuhrhop and W. Helfrich, *Chem. Rev.*, 1993, **93**, 1565–1582.
9 T. Shimizu, M. Masuda and H. Minamikawa, *Chem. Rev.*, 2005, **105**, 1401–1444.
10 Y. Chen, B. Zhu, F. Zhang, Y. Han and Z. Bo, *Angew. Chem., Int. Ed.*, 2008, **47**, 6015–6018.
11 Y. Lin, X. Han, X. Cheng, J. Huang, D. Liang and C. Yu, *Langmuir*, 2008, **24**, 13918–13924.
12 G. Kume, M. Gallotti and G. Nunes, *J. Surfactants Deterg.*, 2008, **11**, 1–11.
13 N. A. Smirnova, *Russ. Chem. Rev.*, 2005, **74**, 129.
14 Y. Lin, X. Han, X. Cheng, J. Huang, D. Liang and C. Yu, *Langmuir*, 2008, **24**, 13918–13924.
15 B. Sohrabi, H. Gharibi, B. Tajik, S. Javadian and M. Hashemianzadeh, *J. Phys. Chem. B*, 2008, **112**, 14869–14876.
16 H. Yin, S. Lei, S. Zhu, J. Huang and J. Ye, *Chem.–Eur. J.*, 2006, **12**, 2825–2835.
17 J. Bhattacharjee, V. Aswal, P. Hassan, R. Pamu, J. Narayanan and J. Bellare, *Soft Matter*, 2012, **8**, 10130–10140.
18 O. Söderman, K. L. Herrington, E. W. Kaler and D. D. Miller, *Langmuir*, 1997, **13**, 5531–5538.
19 K. L. Herrington, E. W. Kaler, D. D. Miller, J. A. Zasadzinski and S. Chiruvolu, *J. Phys. Chem.*, 1993, **97**, 13792–13802.
20 J. B. Huang, B. Y. Zhu, G. X. Zhao and Z. Y. Zhang, *Langmuir*, 1997, **13**, 5759–5761.
21 J.-B. Huang, B.-Y. Zhu, M. Mao, P. He, J. Wang and X. He, *Colloid Polym. Sci.*, 1999, **277**, 354–360.
22 W.-Y. Yu, Y.-M. Yang and C.-H. Chang, *Langmuir*, 2005, **21**, 6185–6193.
23 L. L. Brasher, K. L. Herrington and E. W. Kaler, *Langmuir*, 1995, **11**, 4267–4277.
24 H. Yin, Z. Zhou, J. Huang, R. Zheng and Y. Zhang, *Angew. Chem.*, 2003, **115**, 2238–2241.
25 H. Yin, J. Huang, Y. Gao and H. Fu, *Langmuir*, 2005, **21**, 2656–2659.
26 H. Yin, Y. Lin, J. Huang and J. Ye, *Langmuir*, 2007, **23**, 4225–4230.
27 L. Jiang, K. Wang, M. Deng, Y. Wang and J. Huang, *Langmuir*, 2008, **24**, 4600–4606.
28 Y. Lin, Y. Zhang, Y. Qiao, J. Huang and B. Xu, *J. Colloid Interface Sci.*, 2011, **362**, 430–438.
29 D. Ke, C. Zhan, A. D. Li and J. Yao, *Angew. Chem.*, 2011, **123**, 3799–3803.
30 G. Yu, Y. Ma, C. Han, Y. Yao, G. Tang, Z. Mao, C. Gao and F. Huang, *J. Am. Chem. Soc.*, 2013, **135**, 10310–10313.
31 W. H. Johns and T. R. Bates, *J. Pharm. Sci.*, 1970, **59**, 329–333.
32 D. M. Rock and R. L. MacDonald, *Mol. Pharmacol.*, 1992, **42**, 157–164.
33 G. Giorgi, I. Pini, L. Ceraulo and V. T. Liveri, *J. Mass Spectrom.*, 2011, **46**, 925–932.
34 G. Giorgi, D. Bongiorno, V. T. Liveri, F. Di Gaudio, S. Indelicato, L. Ceraulo and S. Indelicato, *Eur. J. Mass Spectrom.*, 2012, **17**, 525–541.
35 G. Giorgi, L. Ceraulo and V. Turco Liveri, *J. Phys. Chem. B*, 2008, **112**, 1376–1382.
36 J. H. Jung, G. John, K. Yoshida and T. Shimizu, *J. Am. Chem. Soc.*, 2002, **124**, 10674–10675.
37 J. H. Jung, Y. Do, Y. A. Lee and T. Shimizu, *Chem.–Eur. J.*, 2005, **11**, 5538–5544.

